

Stability of Axisymmetric Pendular Rings

Leonid G. Fel¹ and Boris Y. Rubinstein²

¹Department of Civil and Environmental Engineering,

Technion – Israel Institute of Technology, Haifa, 32000, Israel

²Stowers Institute for Medical Research, 1000 E 50th St, Kansas City, MO 64110, USA

Abstract

Based on the Weierstrass representation of second variation we develop a non-spectral theory of stability for isoperimetric problem with minimized and constrained two-dimensional functionals of general type and free endpoints allowed to move along two given planar curves. We apply this theory to the axisymmetric pendular ring between two solid bodies without gravity to determine the stability of menisci with free contact lines. For catenoid and cylinder menisci and different solid shapes we determine the stability domain. The other menisci (unduloid, nodoid and sphere) are considered in a simple setup between two plates. We find the existence conditions of stable unduloid menisci with and without inflection points.

1 Introduction

A capillary surface is an interface separating two non-mixing fluids adjacent to each other. Its shape depends on liquid volume and on boundary conditions (BC) specified at the contact line (CL) where the liquids touch the solid. A pendular ring (PR) is one of the well studied among different types of drops (sessile, pendant [23], *etc.*). It emerges when a small amount of fluid forms a axisymmetric liquid bridge with interface (meniscus) between two axisymmetric solids. A history of the PR problem without gravity shows a remarkable interaction between theoretical physics and pure mathematics and can be traced in two directions: evolution of menisci shapes (including their volume V , surface area S and surface curvature H calculation) and study of their stability.

Delaunay [5] was the first who classified all surfaces of revolution with constant mean curvature (CMC) in his study of the Young-Laplace equation (YLE). These are cylinder (Cyl), sphere (Sph), catenoid (Cat), nodoid (Nod) and unduloid (Und). Later Beer [2] gave analytical solutions of YLE

in elliptic integrals and Plateau [14] supported the theory by experimental observations. For a whole century almost no rigorous results were reported on the computation of H , V and S of PR. In the 1970s Orr *et. al.* [13] gave such formulas for all meniscus types in case of a solid sphere contacting a solid plate. A new insight into the problem was presented recently in [15] for the case of separated solid sphere and plate as a nonlinear eigenvalue equation with a discrete spectrum. The existence of multiple solutions of YLE for given PR volume reported in [15] poses a question of local stability of menisci.

The first step toward the modern theory of PR stability was made by Sturm [17] in appendix to [5], characterizing CMC surfaces as the solutions to isoperimetric problem (**IP**). Such relationship between a second order differential equation and a functional reaching its extremal value was known at the time. The basis of calculus of variations was laid in the 1870s by Weierstrass in his unpublished lectures [22] and extended by Bolza [3] and others. The difficult part of the theory deals with the second variation in vicinity of extremal solutions of the Euler-Lagrange equations (ELE).

The **IP** with fixed endpoints t_1, t_2 was studied first by Weierstrass who derived a determinant equation [22], p. 275, which defines an existence of conjugate points. Later Howe [10] applied Weierstrass' theory to study the PR problem with fixed CL. In the last decades this approach continued to be used in different setups (see, *e.g.*, [6, 8]). Stability of axisymmetric menisci with free CL at solid bodies is a variational **IP** with free endpoints allowed to move along two given planar curves S_1, S_2 .

The **IP** providing $\Xi_0[w] = \min$ with an integrand quadratic in w, w' , linear constraint $\Xi_1[w] = 1$ and fixed BC $w(t_j) = 0$ is related to an eigenvalue problem associated with a linear operator (see [4], Chap. 6). This is true even if the homogeneous (fixed) BC is replaced by any other linear homogeneous BC (Dirichlet, Neumann or mixed) and also is consistent with additional normalization $\Xi_2[w] = \int_{t_2}^{t_1} w^2 dt = 1$, which eliminates an ambiguity of minimizing solution $Aw(t)$ of **IP** with arbitrary constant A . Thus, the **IP** for the functional $\Xi_0[w] + \mu\Xi_1[w] - \lambda\Xi_2[w]$ with two Lagrange multipliers μ, λ and two constraints Ξ_1, Ξ_2 gives rise to the Sturm-Liouville equation (SLE) with real spectrum $\{\lambda_n\}$ and stability criterion: $\min\{\lambda_n\} > 0$. A study of the spectrum $\{\lambda_n\}$ of SLE is a very complicated task for generic curves S_1, S_2 . Such approach was implemented [12] to study the stability of liquid drop with fixed CL.

Spectral theory of linear operators in PR problem with free CL cannot be applied directly since a minimization of $\Xi_0[w]$ with constraint $\Xi_1[w] = 1$ leads to a unique solution in the case of inhomogeneous BC $w(t_j) \neq 0$. In the 1980s Vogel suggested another approach to this problem constructing an associated SLE with Neumann BC instead of Dirichlet BC, and established the stability criterion valid for PR between plates [18, 19]. This method requires to solve the eigenvalue problem and to consider the behavior of the two first minimal eigenvalues $\lambda_{1,2}$. Implementation of this step is extremely difficult task

in the case of Und and Nod menisci. This is why only some exact results for Cat [24], Sph [16] and Und [7] menisci between two plates are known. Investigation of the bridges stability between other surfaces encounters even more difficulties. This was done only for Cyl [20] and (qualitatively) for convex Und and Nod [21] between equal solid spheres. This method [21] allows to consider also a stability with respect to non-axisymmetric perturbations. No results on stability of menisci between other solids (similar or different) are reported.

Based on the Weierstrass representation of second variation we develop a non-spectral theory of stability for **IP** with the minimized $E[x, y]$ and constrained $V[x, y]$ functionals of general type and with free endpoints belonging to generic curves. We apply this theory to PR of arbitrary shape and axisymmetric solid bodies to determine the stability of meniscus with free CL.

The present paper is organized in six sections. In the first part, sections 2, 3, 4, we recall a setup of **IP** and the Weierstrass representation of second variation with the stability criterion for variations with fixed endpoints based on which we derive the stability criterion for free CL in closed form. In section 2 we derive two ELE supplemented with BC (transversality conditions) and find its extremal solution $\bar{x}(t), \bar{y}(t)$ which serves as a functional parameter in formulation of **IP** for second variation $\Xi_0[w] = \delta^2 E[x, y]$ with constraint $\Xi_1[w] = \delta V[x, y] = 0$. In section 3 for the case of fixed endpoints this leads to the Jacobi equation with homogeneous BC $w(t_j) = 0$ for perturbation function $w(t)$. Its fundamental and particular solutions produce the necessary condition of stability (the criterion of conjugate points absence) that generate the stability domain $\text{Stab}_1(t_2, t_1)$ for extremal solution in the $\{t_1, t_2\}$ -plane. In section 4 we derive the expression for $\delta^2 E[x, y]$ as a quadratic form in small perturbations $\delta\tau_j$ of the meniscus endpoints along the curves $S_j(\tau_j)$ and find a domain $\mathbb{Q}(t_2, t_1)$ where this form is positive definite. Finally we find the stability domain $\text{Stab}_2(t_2, t_1)$ for extremal solution with free endpoints as intersection of Stab_1 and \mathbb{Q} .

In the second part, sections 5, 6, this approach is applied to study the stability of axisymmetric PR between solid bodies in absence of gravity. For Cat and Cyl menisci we consider different solid shapes and calculate Stab_2 . Among other new results we verify the solutions for Cat menisci between two plates [24] and Cyl menisci between two spheres [20] obtained in the framework of Vogel's theory. The other menisci are treated in section 6.2 in a simple setup between two plates. We find the existence conditions of stable Und menisci with and without inflection point and verify conclusions [7] on their stability for special contact angles. Stability of Und, Nod and Sph menisci between non-planar bodies will be considered in the separate paper.

2 Stability problem as a variational problem

Let a planar curve C with parametrization $\{x(t), y(t)\}$, $t_1 \leq t \leq t_2$, be given with its endpoints $\{x(t_j), y(t_j)\}$, $j = 1, 2$ allowed to move along two given curves S_j parametrized as $\{X_j(\tau_j), Y_j(\tau_j)\}$, $0 \leq \tau_j \leq \tau_j^*$ (variable τ_j runs along S_j). Consider the first isoperimetric problem (**IP-1**) for the functional $E[x, y]$,

$$E[x, y] = \int_{t_2}^{t_1} E(x, y, x_t, y_t) dt + \sum_{j=1}^2 \int_0^{\tau_j^*} A_j(X_j, Y_j, X_{j,\tau}, Y_{j,\tau}) d\tau, \quad (2.1)$$

with constraint $V[x, y] = 1$ imposed on functional,

$$V[x, y] = \int_{t_2}^{t_1} V(x, y, x_t, y_t) dt + \sum_{j=1}^2 (-1)^j \int_0^{\tau_j^*} B_j(X_j, Y_j, X_{j,\tau}, Y_{j,\tau}) d\tau, \quad (2.2)$$

where we denote $f_t = f' = df/dt$ and $F_{k,t} = F'_k = dF_k/dt$.

The integrands E and V should be positive homogeneous functions of degree one in x_t and y_t , e.g., $E(x, y, kx_t, ky_t) = kE(x, y, x_t, y_t)$, that results in identities stemming from Euler theorem for homogeneous functions,

$$E = \frac{\partial E}{\partial x_t} x_t + \frac{\partial E}{\partial y_t} y_t, \quad A_j = \frac{\partial A_j}{\partial X_{j,\tau_j}} X_{j,\tau_j} + \frac{\partial A_j}{\partial Y_{j,\tau_j}} Y_{j,\tau_j}, \quad (2.3)$$

and similar relations for V and B_j .

We have to find an extremal curve $\bar{C} = \{\bar{x}(t), \bar{y}(t)\}$ with free endpoints $\bar{x}(t_j), \bar{y}(t_j)$ which belong to two given curves S_j such that the functional $E[x, y]$ reaches its minimum while the other functional $V[x, y]$ is constrained.

Define a functional $W[x, y] = E[x, y] - \lambda V[x, y]$ with the Lagrange multiplier λ

$$W[x, y] = \int_{t_2}^{t_1} F(x, y, x_t, y_t) dt - \sum_{j=1}^2 (-1)^j \int_0^{\tau_j^*} G_j(X_j, Y_j, X_{j,\tau}, Y_{j,\tau}) d\tau, \quad (2.4)$$

where $F = E - \lambda V$, $G_1 = \lambda B_1 + A_1$, $G_2 = \lambda B_2 - A_2$. According to (2.3) we have also

$$F = \frac{\partial F}{\partial x_t} x_t + \frac{\partial F}{\partial y_t} y_t, \quad G_j = \frac{\partial G_j}{\partial X_{j,\tau_j}} X_{j,\tau_j} + \frac{\partial G_j}{\partial Y_{j,\tau_j}} Y_{j,\tau_j}. \quad (2.5)$$

Calculate the total variation of the functional, $\mathbb{D}W = \mathbb{D}_0W + \mathbb{D}_1W - \mathbb{D}_2W$,

$$\begin{aligned} \mathbb{D}_0W &= \int_{t_2+\delta t_2}^{t_1+\delta t_1} [F + \Delta_1 F + \Delta_2 F + \dots] dt - \int_{t_2}^{t_1} F dt, \\ \mathbb{D}_jW &= \int_0^{\tau_j^*+\delta\tau_j} G_j d\tau_j - \int_0^{\tau_j^*} G_j d\tau_j, \end{aligned} \quad (2.6)$$

where

$$\begin{aligned}\Delta_1 F &= \frac{\partial F}{\partial x}u + \frac{\partial F}{\partial x_t}u' + \frac{\partial F}{\partial y}v + \frac{\partial F}{\partial y_t}v', \\ \Delta_2 F &= \frac{u^2}{2} \frac{\partial^2 F}{\partial x^2} + uu' \frac{\partial^2 F}{\partial x \partial x_t} + \frac{u'^2}{2} \frac{\partial^2 F}{\partial x_t^2} + \frac{v^2}{2} \frac{\partial^2 F}{\partial y^2} + vv' \frac{\partial^2 F}{\partial y \partial y_t} \\ &+ \frac{v'^2}{2} \frac{\partial^2 F}{\partial y_t^2} + uv \frac{\partial^2 F}{\partial x \partial y} + uv' \frac{\partial^2 F}{\partial x \partial y_t} + u'v \frac{\partial^2 F}{\partial x_t \partial y} + u'v' \frac{\partial^2 F}{\partial x_t \partial y_t},\end{aligned}\tag{2.7}$$

and $\{u(t), v(t)\}$ is a small perturbation in vicinity of curve \bar{C} where the extremum of **IP-1** is reached.

Define a projection of the $\{u(t), v(t)\}$ vector on the normal to the extremal $\{\bar{x}(t), \bar{y}(t)\}$,

$$w(t) = u \bar{y}_t - v \bar{x}_t.\tag{2.8}$$

Represent $\mathbb{D}_0 W$ and $\mathbb{D}_j W$ up to the terms quadratic in $\delta\tau_j, u, v, u', v'$,

$$\begin{aligned}\mathbb{D}_0 W &= \int_{t_2}^{t_1} \Delta_1 F dt + \int_{t_2}^{t_1} \Delta_2 F dt, \quad \mathbb{D}_j W = G_j^* \delta\tau_j + \frac{1}{2} \frac{dG_j^*}{d\tau_j} \delta^2 \tau_j, \\ \frac{dG_j^*}{d\tau_j} &= \frac{\partial G_j^*}{\partial X_j} \frac{dX_j}{d\tau_j} + \frac{\partial G_j^*}{\partial Y_j} \frac{dY_j}{d\tau_j} + \frac{\partial G_j^*}{\partial X_j'} \frac{d^2 X_j}{d\tau_j^2} + \frac{\partial G_j^*}{\partial Y_j'} \frac{d^2 Y_j}{d\tau_j^2},\end{aligned}\tag{2.9}$$

where $G_j^* = G_j$ and $\partial G_j^* / \partial X_j = \partial G_j / \partial X_j$ computed at $\tau_j = \tau_j^*$.

2.1 First variation δW and ELE

Using the terms in (2.9) linear in $\delta\tau_j, u, v$ and u_t, v_t , in expression (2.6) calculate δW

$$\delta W = \int_{t_2}^{t_1} \Delta_1 F dt + G_1^* \delta\tau_1 - G_2^* \delta\tau_2.\tag{2.10}$$

To derive BC for perturbations $u(t_j), v(t_j)$ we have to make them consistent with free endpoints running along the curves S_j

$$\begin{aligned}\bar{x}(t_j) &= X(\tau_j^*), \quad \bar{x}(t_j) + u(t_j) = X(\tau_j^* + \delta\tau_j), \\ \bar{y}(t_j) &= Y(\tau_j^*), \quad \bar{y}(t_j) + v(t_j) = Y(\tau_j^* + \delta\tau_j),\end{aligned}\tag{2.11}$$

resulting in a sequence of equalities: $u(t_j) = \sum_{k=1}^{\infty} u_k(t_j)$ and $v(t_j) = \sum_{k=1}^{\infty} v_k(t_j)$,

$$u_k(t_j) = \frac{1}{k!} \frac{d^k X_j}{d\tau_j^k} \delta^k \tau_j, \quad v_k(t_j) = \frac{1}{k!} \frac{d^k Y_j}{d\tau_j^k} \delta^k \tau_j.\tag{2.12}$$

The function $w(t)$ defined in (2.8) reads at the endpoints,

$$w(t_j) = \eta(t_j, \tau_j^*) \delta\tau_j, \quad \eta(t_j, \tau_j^*) = \bar{y}_t \frac{dX_j}{d\tau_j} - \bar{x}_t \frac{dY_j}{d\tau_j}.\tag{2.13}$$

Denote by $\delta F/\delta z = \partial F/\partial z - \frac{d}{dt}(\partial F/\partial z')$ the variational derivative. Then δW in (2.10) may be written as

$$\delta W = \int_{t_2}^{t_1} \left(u \frac{\delta F}{\delta x} + v \frac{\delta F}{\delta y} \right) dt + \left[u_1 \frac{\partial F}{\partial x'} + v_1 \frac{\partial F}{\partial y'} \right]_{t_2}^{t_1} + G_1^* \delta \tau_1 - G_2^* \delta \tau_2.$$

Substitute $u_1(t_j)$ and $v_1(t_j)$ from (2.12) into the last expression and obtain

$$\delta W = \int_{t_2}^{t_1} \left(u \frac{\delta F}{\delta x} + v \frac{\delta F}{\delta y} \right) dt - \sum_{j=1}^2 (-1)^j \left[\frac{\partial F_j}{\partial x'} \frac{dX_j}{d\tau_j} + \frac{\partial F_j}{\partial y'} \frac{dY_j}{d\tau_j} + G_j^* \right] \delta \tau_j,$$

where $F_j = F$, $\partial F_j/\partial x = \partial F/\partial x$, etc. computed at $t = t_j$. Thus, we arrive at ELE

$$\frac{\partial F}{\partial x} - \frac{d}{dt} \frac{\partial F}{\partial x'} = 0, \quad \frac{\partial F}{\partial y} - \frac{d}{dt} \frac{\partial F}{\partial y'} = 0, \quad (2.14)$$

supplemented by the transversality conditions:

$$\frac{\partial F_2}{\partial x'} \frac{dX_2}{d\tau_2} + \frac{\partial F_2}{\partial y'} \frac{dY_2}{d\tau_2} + G_2^* = 0, \quad \frac{\partial F_1}{\partial x'} \frac{dX_1}{d\tau_1} + \frac{\partial F_1}{\partial y'} \frac{dY_1}{d\tau_1} + G_1^* = 0. \quad (2.15)$$

Solution $\bar{x}(t), \bar{y}(t)$ provides the extremal value of $E[x, y]$ and constraint $V[x, y] = 1$.

Identify $E[x, y]$ as a functional of surface energy of PR and fix its volume by variational constraint $V[x, y] = 1$. Then we arrive at the PR problem [15] in absence of gravity where ELE (2.14) and transversality conditions (2.15) are known as YLE and Young relations. The latter leaves free the values $x(t_j), y(t_j)$ at the endpoints where the meniscus contacts the solid surfaces at the fixed contact angles.

2.2 The Weierstrass representation of second variation $\delta^2 W$

Making use in (2.6) of the terms quadratic in $\delta \tau_j, u, v$ and u', v' , calculate the second variation $\delta^2 W$,

$$\delta^2 W = \int_{t_2}^{t_1} \Delta_2 F dt + \left(\frac{\partial F}{\partial x'} u_2 + \frac{\partial F}{\partial y'} v_2 \right)_{t_2}^{t_1} + \frac{1}{2} \left(\frac{dG_1}{d\tau_1} \delta^2 \tau_1 - \frac{dG_2}{d\tau_2} \delta^2 \tau_2 \right), \quad (2.16)$$

Substituting u_2 and v_2 from (2.12) into the last expression we obtain

$$\delta^2 W = \int_{t_2}^{t_1} \Delta_2 F dt - \frac{1}{2} \sum_{j=1}^2 (-1)^j \left(\frac{\partial F}{\partial x'} \frac{d^2 X_j}{d\tau_j^2} + \frac{\partial F}{\partial y'} \frac{d^2 Y_j}{d\tau_j^2} + \frac{dG_j}{d\tau_j} \right) \delta^2 \tau_j.$$

Denote $\delta_B^2 W = \int_{t_2}^{t_1} \Delta_2 F dt$ and following Weierstrass [22], pp.132-134 (see also Bolza [3], p.206) represent $\delta_B^2 W$ in terms of small perturbation $\{u(t), v(t)\}$ of the extremal curve $\{\bar{x}(t), \bar{y}(t)\}$ and $w(t)$,

$$\delta_B^2 W[x, y] = \frac{1}{2} \Xi_0[w] + \frac{1}{2} [Lu_1^2 + 2Mu_1v_1 + Nv_1^2] \Big|_{t_2}^{t_1}, \quad (2.17)$$

$$\Xi_0[w] = \int_{t_2}^{t_1} [H_1 w'^2 + H_2 w^2] dt, \quad M = F_{xy'} + \bar{x}_t \bar{y}_{tt} H_1 = F_{yx'} + \bar{y}_t \bar{x}_{tt} H_1, \quad (2.18)$$

$$L = F_{xx'} - \bar{y}_t \bar{y}_{tt} H_1, \quad N = F_{yy'} - \bar{x}_t \bar{x}_{tt} H_1, \quad H_1 = \frac{F_{x'x'}}{\bar{y}_t^2} = \frac{F_{y'y'}}{\bar{x}_t^2} = -\frac{F_{x'y'}}{\bar{x}_t \bar{y}_t},$$

$$H_2 = \frac{F_{xx} - \bar{y}_{tt}^2 H_1 - L_t}{\bar{y}_t^2} = \frac{F_{yy} - \bar{x}_{tt}^2 H_1 - N_t}{\bar{x}_t^2} = -\frac{F_{xy} + \bar{x}_{tt} \bar{y}_{tt} H_1 - M_t}{\bar{x}_t \bar{y}_t}.$$

Substituting (2.12) and (2.9) into (2.16) we obtain,

$$\delta^2 W = \delta_B^2 W + \xi_1 \delta^2 \tau_1 - \xi_2 \delta^2 \tau_2, \quad \text{where} \quad (2.19)$$

$$2\xi_j = \frac{\partial F_j}{\partial x'} \frac{d^2 X_j}{d\tau_j^2} + \frac{\partial F_j}{\partial y'} \frac{d^2 Y_j}{d\tau_j^2} + \frac{\partial G_j}{\partial X_j} \frac{dX_j}{d\tau_j} + \frac{\partial G_j}{\partial Y_j} \frac{dY_j}{d\tau_j} + \frac{\partial G_j}{\partial X_j'} \frac{d^2 X_j}{d\tau_j^2} + \frac{\partial G_j}{\partial Y_j'} \frac{d^2 Y_j}{d\tau_j^2}.$$

Substitute $u_1(t_j), v_1(t_j)$ from (2.12) into (2.17) and combine it with (2.19), and find,

$$\delta^2 W = \frac{1}{2} \Xi_0[w] + K_1 \delta^2 \tau_1 - K_2 \delta^2 \tau_2, \quad (2.20)$$

$$2K_j = 2\xi_j + L(t_j) \left(\frac{dX_j}{d\tau_j} \right)^2 + 2M(t_j) \frac{dX_j}{d\tau_j} \frac{dY_j}{d\tau_j} + N(t_j) \left(\frac{dY_j}{d\tau_j} \right)^2. \quad (2.21)$$

3 Homogeneous boundary conditions: fixed endpoints

Study the stability of the extremal curve $\{\bar{x}(t), \bar{y}(t)\}$ w.r.t. small fluctuations in two different cases considered separately; the first case corresponds to the perturbation of the extremal curve in the interval (t_2, t_1) for the fixed endpoints,

$$u(t_j) = v(t_j) = w(t_j) = 0, \quad j = 1, 2. \quad (3.1)$$

The second case is when at least one endpoint is free and allowed to run along given curves S_j is discussed in section 4. Start with the second isoperimetric problem (**IP-2**) associated with perturbations $\{u(t), v(t)\}$ in the vicinity of $\{\bar{x}(t), \bar{y}(t)\}$ with BC (3.1). Following Bolza [3], p.215, write the constraint for $V[x, y]$,

$$\Xi_1[w] = \int_{t_2}^{t_1} H_3 w dt = 0, \quad \begin{cases} H_3 = V_{xy'} - V_{x'y} + H_4(\bar{x}_t \bar{y}_{tt} - \bar{y}_t \bar{x}_{tt}), \\ H_4 = V_{x'x'} \bar{y}_t^{-2} = V_{y'y'} \bar{x}_t^{-2} = -V_{x'y'} \bar{x}_t^{-1} \bar{y}_t^{-1}, \end{cases} \quad (3.2)$$

which involves perturbation w . For PR problem we have $V = x^2 y'$, $B_j = X_j^2 Y_j'$, leading to $H_3 = \bar{x}$, which substantially simplifies the computation (see section 5).

Substitute (3.1) into (2.17) and arrive at the classical **IP** with the second variation $\Xi_0[w]$ treated in the framework of Weierstrass' theory (see [3], Chap. 6). Analyzing the problem with functional $\Xi_2[w] = \Xi_0[w] + 2\mu \Xi_1[w]$,

$$\Xi_2[w] = \int_{t_2}^{t_1} \mathcal{H}(t, w, w') dt, \quad \mathcal{H}(t, w, w') = H_1 w'^2 + H_2 w^2 + 2\mu H_3 w, \quad (3.3)$$

and the Lagrange multiplier μ , write ELE for the function $w(t)$ as an inhomogeneous Jacobi equation with BC given in (3.1)

$$(H_1 w')' - H_2 w = \mu H_3, \quad w(t_1) = w(t_2) = 0. \quad (3.4)$$

The point $t'_2 \neq t_2$ is called *conjugate* to the point t_2 , if (3.4) has a solution $\bar{w}(t)$ such that $\bar{w}(t_2) = \bar{w}(t'_2) = 0$, but is not identically zero. According to Bolza [3], pp.217-220, the following set of conditions is sufficient for the functional (3.3) to have a weak minimum for the solution $\bar{w}(t)$ of equations (3.4):

$$a) H_1(t) > 0, \quad b) \text{ the interval } [t_2, t_1] \text{ contains no points conjugate to } t_2. \quad (3.5)$$

In fact, conditions (3.5) provide a strong minimum because the Weierstrass function $\mathcal{E}(t, w, w', f) = \mathcal{H}(t, w, f) - \mathcal{H}(t, w, w') + (w' - f)\mathcal{H}_{w'}(t, w, w')$ for the functional $\Xi_2[w]$ in (3.3) is positive,

$$\mathcal{E}(t, w, w', f) = H_1 [f(t) - w'(t)]^2, \quad \text{for } f(t) \neq w'(t). \quad (3.6)$$

Weierstrass [22], p. 275, gave another version of conjugate points non-existence condition. Assume that $\bar{w}_1(t)$ and $\bar{w}_2(t)$ are fundamental solutions of homogeneous Jacobi equation, then the particular solution $\mu\bar{w}_3(t)$ of inhomogeneous Jacobi equation (3.4) may be found by standard procedure

$$\bar{w}_3(t) = \bar{w}_2 \int^t \frac{\bar{w}_1 H_3}{H_1 W_r} ds - \bar{w}_1 \int^t \frac{\bar{w}_2 H_3}{H_1 W_r} ds, \quad W_r = \bar{w}_1 \bar{w}'_2 - \bar{w}_2 \bar{w}'_1, \quad (3.7)$$

where W_r denotes the Wronskian for fundamental solutions. Find W_r assuming that \bar{w}_1 is known and the second fundamental solution reads $\bar{w}_2 = U(t)\bar{w}_1$. Substitute it into (3.4) with $\mu = 0$ and obtain

$$\frac{d}{dt} \left(H_1 \bar{w}_1^2 \frac{dU}{dt} \right) = 0, \quad \frac{dU}{dt} = \frac{g}{H_1 \bar{w}_1^2}, \quad W_r = \bar{w}_1^2 \frac{dU}{dt} = \frac{g}{H_1}, \quad (3.8)$$

where g is an integration constant. The fundamental solutions w_j also can be expressed as $w_j = y'(\partial x / \partial \alpha_j) - x'(\partial y / \partial \alpha_j)$, $j = 1, 2$, where α_j denotes the integration constant emerging from ELE (see Bolza [3], p.219). Making use of the last expression in (3.7) we arrive at

$$g\bar{w}_3 = \bar{w}_2 J_1 - \bar{w}_1 J_2, \quad g\bar{w}'_3 = \bar{w}'_2 J_1 - \bar{w}'_1 J_2, \quad g\bar{w}''_3 = \bar{w}''_2 J_1 - \bar{w}''_1 J_2 + \frac{gH_3}{H_1}, \quad (3.9)$$

where $J_k = \int^t H_3 \bar{w}_k ds$. Following Weierstrass [22] introduce the matrix,

$$D(t_2, t') = \begin{pmatrix} \bar{w}_1(t_2) & \bar{w}_2(t_2) & \bar{w}_3(t_2) \\ \bar{w}_1(t') & \bar{w}_2(t') & \bar{w}_3(t') \\ J_1(t') - J_1(t_2) & J_2(t') - J_2(t_2) & J_3(t') - J_3(t_2) \end{pmatrix}. \quad (3.10)$$

Then the condition of non-existence of conjugate points reads (see [22], p.275),

$$\Delta(t_2, t') \neq 0, \quad t_2 < t' < t_1, \quad \Delta(t_2, t_1) = \det D(t_2, t_1). \quad (3.11)$$

Bolza in [3], p.223, gave a more general condition of non-existence of conjugate points,

$$\Delta(t'', t') \neq 0, \quad t_2 < t' < t'' < t_1, \quad (3.12)$$

making the Jacobi condition (3.5b) symmetric with respect to the endpoints t_2 and t_1 . Write a determinant equation $\Delta(t_2, t_1) = 0$ as follows,

$$\begin{aligned} \Delta(t_2, t_1) = & I_3 [\bar{w}_1(t_2)\bar{w}_2(t_1) - \bar{w}_1(t_1)\bar{w}_2(t_2)] + [I_1\bar{w}_2(t_1) - I_2\bar{w}_1(t_1)]\bar{w}_3(t_2) \\ & + [I_2\bar{w}_1(t_2) - I_1\bar{w}_2(t_2)]\bar{w}_3(t_1), \quad \text{where } I_k = J_k(t_1) - J_k(t_2). \end{aligned} \quad (3.13)$$

If $\bar{w}_1(t)$ and $\bar{w}_2(t)$ are continuous functions then solution of equation $\Delta(t_2, t_1) = 0$ describes a continuous curve $\mathcal{D}(t_2, t_1)$ of conjugated points.

Another important requirement is to guarantee that the extremal $\{\bar{x}(t), \bar{y}(t)\}$ does not intersect with the curves S_j . In the case of the PR this requirement provides the meniscus existence condition given by the constant sign of $\eta(t_j, \tau_j^*)$. Define the lines $t_j = t_j^\bullet$ in $\{t_1, t_2\}$ -plane where $\eta(t_j^\bullet, \tau_j^*) = 0$.

Consider a point $M_1 = (a, b)$ in the lower halfplane $\{t_2 < t_1\}$ and two more points: $M_2 = (a, a)$ and $M_3 = (b, b)$. Call a point M_1 the Jacobi point if the line M_1M_2 does not intersect both $\mathcal{D}(t_2, t_1)$ and $t_2 = t_2^\bullet$, and M_1M_3 does not intersect both $\mathcal{D}(t_2, t_1)$ and $t_1 = t_1^\bullet$. Define a set $\mathbb{J}(t_2, t_1)$ as a union of points M_1

$$\mathbb{J}(t_2, t_1) = \left\{ (a, b) \left| \begin{array}{l} \Delta(t, a) \neq 0, \Delta(b, t) \neq 0, \quad t_2 < b \leq t \leq a < t_1, \\ \eta(t_2, \tau_2^*) \neq 0, \quad t_2^\bullet < b \leq t_2 \leq a < t_1, \\ \eta(t_1, \tau_1^*) \neq 0, \quad t_2 < b \leq t_1 \leq a < t_1^\bullet. \end{array} \right. \right\} \quad (3.14)$$

representing an open domain in $\{t_1, t_2\}$ -plane. Combining (3.5 a,b) and (3.14) define a stability set as intersection set

$$\text{Stab}_1(t_2, t_1) = \mathbb{J}(t_2, t_1) \cap \mathbb{L}(t_2, t_1), \quad \mathbb{L}(t_2, t_1) = \{(t_2, t_1) | H_1(t) > 0, t \in [t_2, t_1]\} \quad (3.15)$$

where the set $\mathbb{L}(t_2, t_1)$ comprises the points satisfying Legendre's criterion (3.5a).

4 Inhomogeneous boundary conditions: free endpoints

Consider the case when the extremal $\{\bar{x}(t), \bar{y}(t)\}$ is perturbed at the interval $[t_2, t_1]$ including both endpoints. The case of one free and one fixed endpoints will follow as a corollary. The nonintegral term in (2.17) is fixed and in general case it does not vanish; the same is true for (2.20). It is worth to mention that any other BC, e.g., the Neumann BC $w'(t_j) = 0$ in [18] or mixed BC $g_1 w'(t_j) + g_0 w(t_j) = 0$ in [12], leads to changes in $u(t_j), v(t_j)$ and requires variation of the nonintegral term in (2.17).

From physical point of view BC (2.13) requires that *the endpoints of perturbed meniscus* $\{\bar{x} + u, \bar{y} + v\}$ *always belong to the solid surfaces*. These claims are justified from mathematical standpoint:

- The second order Jacobi equation (3.4) for perturbation w admits no more than two BC.
- The perturbed meniscus $\{\bar{x} + u, \bar{y} + v\}$ may not provide the extremum for $W[x, y]$ even if $\{u, v\}$ do provide the extremum for $\delta^2 W[x, y]$.

Following an ideology of stability theory we have to find when $\delta^2 W$ is positive definite in vicinity of the extremal curve constrained by (2.2). Since the only varying part in (2.20) is the functional $\Xi_0[w]$, this brings us to **IP-2** with one indeterminate function $w(t)$: find the extremal $\bar{w}(t)$ providing $\Xi_0[w]$ to be positive definite in vicinity of $\bar{w}(t)$ and preserving $\Xi_1[w]$. Inhomogeneity of BC requires to answer two questions:

$$\text{When is } \Xi_0[w] \text{ positive definite in vicinity of } \bar{w}(t) \text{ for the fixed } \delta\tau_j ? \quad (4.1)$$

$$\text{When does } \Xi_0[\bar{w}] \text{ reach a positive value as a function of displacements } \delta\tau_j ? \quad (4.2)$$

Start with (4.1) and consider the necessary conditions for functional $\Xi_0[w]$ to be positive definite in vicinity of extremal perturbation $\bar{w}(t)$ for the fixed $\delta\tau_j$ and preserving $\Xi_1[w]$. Let us prove that they coincide with those conditions (3.5) for the functional $E[x, y]$ to be positive definite in vicinity of extremal solution $\{\bar{x}(t), \bar{y}(t)\}$ for the fixed endpoints and preserving $V[x, y]$.

For this purpose we ignore a fact that $\Xi_0[w]$ is a second variation, satisfying the relations (2.18), and instead, we treat the analysis of (2.18) as independent problem. Represent w in a vicinity of extremal perturbation \bar{w} ,

$$w(t) = \bar{w}(t) + \varepsilon(t), \quad \varepsilon(t_1) = \varepsilon(t_2) = 0, \quad \Xi_1[\varepsilon] = \int_{t_2}^{t_1} H_3 \varepsilon dt = 0, \quad (4.3)$$

where a perturbation ε preserves both BC (2.13) and the constraint (3.2). Find the first and second variations of functional $\Xi_2[w]$ defined in (3.3),

$$\delta\Xi_2[w] = 2 \int_{t_2}^{t_1} \left[- (H_1 \bar{w}')' + H_2 \bar{w} + \mu H_3 \right] \varepsilon dt, \quad \delta^2 \Xi_2[w] = \int_{t_2}^{t_1} [H_1 \varepsilon'^2 + H_2 \varepsilon^2] dt.$$

The first variation $\delta\Xi_2[w]$ vanishes at the extremal \bar{w} satisfying the inhomogeneous Jacobi equation (3.4). Regarding the second variation $\delta^2 \Xi_2[w]$, it completely coincides with $\Xi_0[w]$ as well as BC and volume constraint (4.3) are coinciding with similar BC (3.1) and constraint (3.2) in the **IP** with fixed endpoints (section 3). This coincidence implies the necessary conditions (3.5) for $\Xi_0[w]$ to be positive definite in vicinity of extremal \bar{w} for the fixed $\delta\tau_j$.

Consider (4.2) and write a general solution \bar{w} of equation (3.4) built upon the fundamental solutions \bar{w}_1, \bar{w}_2 of homogeneous equation, and particular solution of inhomogeneous equation \bar{w}_3 ,

$$\bar{w}(t) = C_1 \bar{w}_1(t) + C_2 \bar{w}_2(t) + \mu \bar{w}_3(t). \quad (4.4)$$

Inserting (4.4) into BC (2.13) and into constraint (3.2) we obtain three linear equations,

$$\bar{w}_1(t_j)C_1 + \bar{w}_2(t_j)C_2 + \bar{w}_3(t_j)\mu = \bar{w}(t_j), \quad I_1C_1 + I_2C_2 + I_3\mu = 0, \quad (4.5)$$

which are uniquely solvable (see [3], p.220) if $\Delta(t_2, t_1) \neq 0$ and have nonzero solutions when at least one of $\bar{w}(t_j)$ is nonzero,

$$C_j = m_{j1}\delta\tau_1 + m_{j2}\delta\tau_2, \quad j = 1, 2, \quad \mu = m_{31}\delta\tau_1 + m_{32}\delta\tau_2. \quad (4.6)$$

Substitute (4.6) into (4.5) and find two equations with matrix $D(t_2, t_1)$ defined in (3.10),

$$D(t_2, t_1)\mathbf{M}_j = \mathbf{N}_j, \quad \mathbf{M}_j = \begin{pmatrix} m_{1j} \\ m_{2j} \\ m_{3j} \end{pmatrix}, \quad \mathbf{N}_1 = \begin{pmatrix} 0 \\ \eta_1 \\ 0 \end{pmatrix}, \quad \mathbf{N}_2 = \begin{pmatrix} \eta_2 \\ 0 \\ 0 \end{pmatrix},$$

where $\eta_j = \eta(t_j, \tau_j^*)$ and $\bar{w}_i(t_j) = \bar{w}_{ij}$. Then $m_{j1} = \eta_1\beta_{j1}/\Delta$, $m_{j2} = \eta_2\beta_{j2}/\Delta$, and

$$\begin{aligned} \beta_{11} &= I_3\bar{w}_{22} - I_2\bar{w}_{32}, & \beta_{21} &= I_1\bar{w}_{32} - I_3\bar{w}_{12}, & \beta_{31} &= I_2\bar{w}_{12} - I_1\bar{w}_{22}, \\ \beta_{12} &= I_2\bar{w}_{31} - I_3\bar{w}_{21}, & \beta_{22} &= I_3\bar{w}_{11} - I_1\bar{w}_{31}, & \beta_{32} &= I_1\bar{w}_{21} - I_2\bar{w}_{11}. \end{aligned}$$

Substituting (4.6) into (4.4), represent $\bar{w}(t)$ as follows

$$\bar{w}(t) = A_1(t)\delta\tau_1 + A_2(t)\delta\tau_2, \quad A_j(t) = \frac{\eta_j B_j(t)}{\Delta(t_2, t_1)}, \quad B_j(t) = B_j(t, t_2, t_1), \quad (4.7)$$

$$B_1(t) = - \begin{vmatrix} \bar{w}_1(t) & \bar{w}_2(t) & \bar{w}_3(t) \\ \bar{w}_1(t_2) & \bar{w}_2(t_2) & \bar{w}_3(t_2) \\ I_1 & I_2 & I_3 \end{vmatrix}, \quad B_2(t) = \begin{vmatrix} \bar{w}_1(t) & \bar{w}_2(t) & \bar{w}_3(t) \\ \bar{w}_1(t_1) & \bar{w}_2(t_1) & \bar{w}_3(t_1) \\ I_1 & I_2 & I_3 \end{vmatrix}.$$

According to (2.13) we have, $B_1(t_2) = B_2(t_1) = 0$, $B_j(t_j) = \Delta(t_2, t_1)$, and its expression is given in (3.13). Straightforward calculation of determinant's derivatives gives

$$\begin{aligned} H_1(t_2)B_1'(t_2) &= -H_1(t_1)B_2'(t_1) = I_1(t_1)I_2(t_2) - I_1(t_2)I_2(t_1) + gI_3, \\ gB_1'(t_1) &= [I_2\bar{w}_1(t_2) - I_1\bar{w}_2(t_2)] [I_2\bar{w}'_1(t_1) - I_1\bar{w}'_2(t_1)] \\ &\quad - H_1(t_1)B_2'(t_1)[\bar{w}_1(t_2)\bar{w}'_2(t_1) - \bar{w}_2(t_2)\bar{w}'_1(t_1)], \\ gB_2'(t_2) &= [I_2\bar{w}_1(t_1) - I_1\bar{w}_2(t_1)] [I_2\bar{w}'_1(t_2) - I_1\bar{w}'_2(t_2)] \\ &\quad - H_1(t_2)B_1'(t_2)[\bar{w}_1(t_1)\bar{w}'_2(t_2) - \bar{w}_2(t_1)\bar{w}'_1(t_2)], \end{aligned} \quad (4.8)$$

where $B_j'(t_k) \equiv dB_j(t, t_2, t_1)/dt$ computed at $t = t_k$. Formula (2.17) together with equation (3.4) allows to express $\delta^2 W[x, y]$ in a simple form. Multiplying (3.4) by \bar{w} and integrating by parts we obtain

$$\int_{t_2}^{t_1} [H_1(t)\bar{w}'^2(t) + H_2(t)\bar{w}^2(t)] dt - H_1(t)\bar{w}(t)\bar{w}'(t)|_{t_2}^{t_1} = 0.$$

Combining the last equality with (2.20) and (2.21) we arrive at

$$\delta^2 W = \frac{1}{2} [H_1 \bar{w} \bar{w}' + Lu^2 + 2Muv + Nv^2] \Big|_{t_2}^{t_1} + \xi_1 \delta^2 \tau_1 - \xi_2 \delta^2 \tau_2, \quad (4.9)$$

where ξ_j are defined in (2.19). Substituting (2.12, 4.7) into (4.9) and using (4.8), we obtain

$$\delta^2 W = Q_{11} (\delta \tau_1)^2 + 2Q_{12} \delta \tau_1 \delta \tau_2 + Q_{22} (\delta \tau_2)^2, \quad (4.10)$$

$$\begin{aligned} Q_{11}(t_2, t_1) &= \frac{\eta_1^2 P_{11}}{2\Delta} + K_1, & P_{11} &= H_1(t_1) B_1'(t_1), \\ Q_{22}(t_2, t_1) &= \frac{\eta_2^2 P_{22}}{2\Delta} - K_2, & P_{22} &= -H_1(t_2) B_2'(t_2), \\ Q_{12}(t_2, t_1) &= \frac{\eta_1 \eta_2 P_{12}}{2\Delta}, & P_{12} &= P_{21} = H_1(t_1) B_2'(t_1), \end{aligned} \quad (4.11)$$

where $\eta_j = \eta(t_j, \tau_j^*)$ and $K_j = K_j(t_j, \tau_j^*)$ are defined in (2.13) and (2.21), respectively.

Using BC (2.11): $\bar{x}(t_j) = X(\tau_j^*)$, $\bar{y}(t_j) = Y(\tau_j^*)$, the matrix elements Q_{ij} may be represented as functions of t_2, t_1 only. The necessary conditions to have $\delta^2 W \geq 0$ are given by three inequalities,

$$Q_{11}(t_2, t_1) \geq 0, \quad Q_{22}(t_2, t_1) \geq 0, \quad Q_{33}(t_2, t_1) = Q_{11} Q_{22} - Q_{12}^2 \geq 0. \quad (4.12)$$

One of the two first inequalities in (4.12) is redundant but we leave it for the symmetry considerations.

Inequalities (4.12) provide an answer to the question (4.2). Define three different sets $\mathbb{Q}_j(t_2, t_1)$

$$\mathbb{Q}_j(t_2, t_1) := \{(a, b) \mid (a, b) \in \{t_2 < t_1\}, Q_{jj}(t_2, t_1) \geq 0\}, \quad (4.13)$$

and the intersection set $\mathbb{Q}(t_2, t_1) := \mathbb{Q}_1(t_2, t_1) \cap \mathbb{Q}_2(t_2, t_1) \cap \mathbb{Q}_3(t_2, t_1)$.

Summarizing answers to both questions (4.1, 4.2) we conclude that the necessary conditions of stability of extremal $\bar{w}(t)$ with BC comprise (3.5), (3.11), (3.15) and (4.11):

$$\text{Stab}_2(t_2, t_1) = \text{Stab}_1(t_2, t_1) \cap \mathbb{Q}(t_2, t_1), \quad \text{Stab}_2(t_2, t_1) \subseteq \text{Stab}_1(t_2, t_1). \quad (4.14)$$

The conditions (4.12) cannot determine the extremal solution stability in case when the determinant Q_{33} in (4.12) vanishes. Indeed, we have in (4.10)

$$\delta^2 W = \left(\sqrt{Q_{11}} \delta \tau_1 + \sqrt{Q_{22}} \delta \tau_2 \right)^2, \quad Q_{33}(t_2, t_1) = 0. \quad (4.15)$$

Thus, there exists a non empty set of perturbations $\delta \tau_1, \delta \tau_2$ such that $\sqrt{Q_{11}} \delta \tau_1 + \sqrt{Q_{22}} \delta \tau_2 = 0$, which does not affect the second variation, *i.e.*, $\delta^2 W = 0$. This limitation of the Weierstrass representation may be resolved by studying the higher variations, $\delta^3 W$ and $\delta^4 W$, which is beyond the scope of the present manuscript.

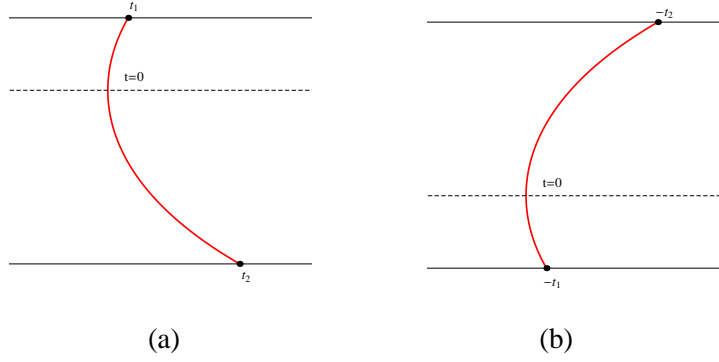


Figure 1: Sketches of menisci between two plates showing the endpoints (a) t_1, t_2 and (b) $-t_2, -t_1$.

Consider two menisci related by symmetry reflection $t_2 \rightarrow -t_1, t_1 \rightarrow -t_2$ w.r.t. a midline between two solids and normal to the curve $\{\bar{x}(t), \bar{y}(t)\}$ at the point $t = 0$ (or to continuation of curve if $0 \notin [t_2, t_1]$) as shown in Figure 1. It is easy to conclude that the stability conditions (4.12) serve for both menisci simultaneously,

$$Q_{ii}(-t_1, -t_2) = Q_{jj}(t_2, t_1), \quad i \neq j = 1, 2; \quad Q_{12}(-t_1, -t_2) = Q_{12}(t_2, t_1). \quad (4.16)$$

Consider a symmetric setup: $t_1 = -t_2 = t$, when two solid bodies are similar and separated by a reflection plane located in the midpoint of the meniscus at $t = 0$. Then due to (4.16) the necessary conditions (4.12) read

$$Q_{11}(-t, t) = Q_{22}(-t, t) \geq 0, \quad Q_{33}(-t, t) = Q_{11}^2(-t, t) - Q_{12}^2(-t, t) \geq 0. \quad (4.17)$$

Expression (4.10) and conditions (4.12) encompass the case when the extremal curve is perturbed at interval $[t_2, t_1]$ including only one endpoint (say, t_1) while another is left fixed. Here, instead of (4.10, 4.12) we have $\delta^2 W = Q_{11} (\delta\tau_1)^2$, $Q_{11}(t_2, t_1) \geq 0$.

5 Application to the problem of pendular rings

Apply our approach to study the stability of axisymmetric PR between solid bodies in absence of gravity. The axial symmetry of bodies is assumed along z -axis (see Figure 2). The shapes of meniscus $\{r(\phi), z(\phi)\}$ and two solid bodies $\{R_j(\psi_j), Z_j(\psi_j)\}$ are given in cylindrical coordinates, *i.e.*, the following correspondence holds,

$$x \rightarrow r, \quad y \rightarrow z, \quad X_j \rightarrow R_j, \quad Y_j \rightarrow Z_j, \quad t \rightarrow \phi, \quad \tau_j \rightarrow \psi_j.$$

The filling angle ψ_j along the j solid-liquid interface is chosen to satisfy $0 \leq \psi_j \leq \infty$ for unbounded solid bodies (semispace with planar boundary, paraboloid, catenoid) and $0 \leq \psi_j < \infty$ for bounded solid bodies (sphere, prolate and oblate ellipsoids).

The functional W and its integrands in (2.4) read

$$W = \int_{\phi_2}^{\phi_1} F(r, r', z, z') d\phi - \sum_{j=1}^2 (-1)^j \int_0^{\psi_j^*} G_j d\psi_j, \quad F = \left[\gamma_{lv} \sqrt{r'^2 + z'^2} - \frac{\lambda r z'}{2} \right] r, \\ G_j = \left[\frac{\lambda R_j Z'_j}{2} - (-1)^j (\gamma_{ls_j} - \gamma_{vs_j}) \sqrt{R_j'^2 + Z_j'^2} \right] R_j, \quad (5.1)$$

where coefficients γ_{lv} , γ_{ls_j} and γ_{vs_j} , $j = 1, 2$, describe surface energy density at three interfaces: liquid-vapor, solid-vapor and solid-liquid for the upper ($j = 1$) and lower ($j = 2$) solid bodies. The two ELE

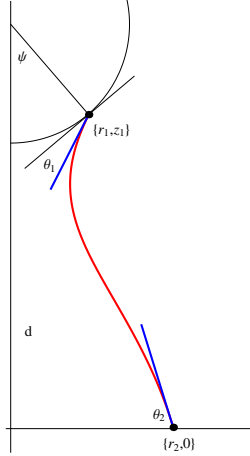


Figure 2: A sketch of meniscus between plane and sphere showing the contact angles θ_1, θ_2 , filling angle ψ and coordinates of the endpoints.

(2.14) are reduced to a single YLE

$$2H = \frac{z'}{r(r'^2 + z'^2)^{1/2}} + \frac{z''r' - z'r''}{(r'^2 + z'^2)^{3/2}}, \quad H = \frac{\lambda}{2\gamma_{lv}}, \quad (5.2)$$

where H stands for the meniscus mean curvature. The transversality conditions (2.15) are known as the Young relations for the contact angle θ_j of the meniscus with the j -th solid body: $\cos \theta_j + (\gamma_{ls_j} - \gamma_{vs_j})/\gamma_{lv} = 0$. According to (2.13) the quantity $\eta_j = \eta(\phi_j, \psi_j^*)$ is given by

$$\eta_j = \bar{z}'(\phi_j)R'(\psi_j^*) - \bar{r}'(\phi_j)Z'(\psi_j^*). \quad (5.3)$$

Define a contact angle θ_j between meniscus and solid body as follows

$$\theta_j = (-1)^{j-1} \left(\arctan \frac{\bar{z}'(\phi_j)}{\bar{r}'(\phi_j)} - \arctan \frac{Z'(\psi_j^*)}{R'(\psi_j^*)} \right), \quad (5.4)$$

where $0 \leq \arctan(\bar{z}'/\bar{r}'), \arctan(Z'/R') \leq \pi$. The contact angle θ_j vanishes when $\bar{z}'/\bar{r}' = Z'/R'$, i.e., $\eta_j = 0$, which manifests meniscus' nonexistence at a critical angle ϕ_j^\bullet in accordance with (3.14)

$$\bar{z}'(\phi_j^\bullet)R'(\psi_j^*) - \bar{r}'(\phi_j^\bullet)Z'(\psi_j^*) = 0, \quad \bar{r}(\phi_j^\bullet) - R(\psi_j^*) = 0. \quad (5.5)$$

Rescale the integrands in (2.4) by $2\gamma_{lv}|H|$ and deal henceforth with expressions,

$$F = \left[\sqrt{r'^2 + z'^2} - \frac{S_H}{2} r z' \right] r, \quad G_j = \left[\frac{S_H}{2} R_j Z_j' + (-1)^j \cos \theta_j \sqrt{R_j'^2 + Z_j'^2} \right] R_j, \quad (5.6)$$

where $S_H = \text{sign}H$. Straightforward calculation in (2.21) gives an expression for K_j ,

$$K_j = U_j \eta_j, \quad U_j = -\frac{R_j}{2\sqrt{\bar{r}_j'^2 + \bar{z}_j'^2}} \left(\frac{\bar{z}_j'' R_j' - \bar{r}_j'' Z_j'}{\bar{r}_j'^2 + \bar{z}_j'^2} - \frac{Z_j'' R_j' - R_j'' Z_j'}{R_j'^2 + Z_j'^2} \right), \quad (5.7)$$

where $\bar{f}_j' = \bar{f}'(\phi_j)$, $\bar{f}_j'' = \bar{f}''(\phi_j)$. Combining (5.7, 4.11) write expressions for $Q_{ij}(\phi_2, \phi_1)$,

$$Q_{11} = \eta_1 \left(\frac{\eta_1 P_{11}}{2\Delta} + U_1 \right), \quad Q_{22} = \eta_2 \left(\frac{\eta_2 P_{22}}{2\Delta} - U_2 \right), \quad Q_{12} = \frac{\eta_1 \eta_2 P_{12}}{2\Delta}, \quad (5.8)$$

that results in $Q_{33} \propto \eta_1 \eta_2$ and according to (4.16) we have $U_j(-\phi, \psi^*) = U_j(\phi, \psi^*)$. Thus, stability domain $\text{Stab}_2(\phi_1, \phi_2)$ of liquid meniscus of any type has boundaries including meniscus nonexistence lines $\phi_j = \phi_j^\bullet$ given by (5.5).

Find formulas for H_j in (3.4) by substituting (5.6) into (2.18, 3.2) and obtain

$$H_1 = \frac{\bar{r}}{(\bar{r}'^2 + \bar{z}'^2)^{3/2}}, \quad H_2 = \frac{(H_1 \bar{r}'')'}{\bar{r}'}, \quad H_3 = \bar{r}, \quad (H_1 w')' \bar{r}' - (H_1 \bar{r}'')' w = \mu \bar{r}' \bar{r}. \quad (5.9)$$

Fundamental solutions of equation (5.9) read,

$$\bar{w}_1 = \bar{r}'(\phi), \quad \bar{w}_2 = E(\phi) \bar{r}'(\phi), \quad E(\phi) = g \int \frac{dt}{H_1 \bar{r}'^2} = g \int \frac{(\bar{r}'^2 + \bar{z}'^2)^{3/2} dt}{\bar{r}'^2 \bar{r}}.$$

5.1 Pendular rings with zero curvature

For $H = 0$ the first Delaunay's type, *catenoid* (Cat) appears from (5.2),

$$\bar{r} = \sec \phi, \quad \bar{z} = \ln \frac{\cos \phi}{1 - \sin \phi} + C, \quad \frac{\bar{z}'}{\bar{r}'} = \cot \phi, \quad \bar{r}'^2 + \bar{z}'^2 = \bar{r}^4, \quad (5.10)$$

where C is the constant determined from the BC. Entries in (2.17) read,

$$H_1 = \frac{1}{\bar{r}^5}, \quad H_2 = -4 \frac{\bar{r}^2 - 1}{\bar{r}^5}, \quad L = \frac{\bar{r}^3 \bar{r}' - \bar{z}' \bar{z}''}{\bar{r}^5}, \quad N = -\frac{\bar{r}' \bar{r}''}{\bar{r}^5}, \quad M = \frac{\bar{z}' \bar{r}''}{\bar{r}^5}. \quad (5.11)$$

Note that $H_1(\phi)$ is always positive, therefore the set $\mathbb{L}(\phi_1, \phi_2)$ is given by the whole lower halfplane $\{\phi_2 < \phi_1\}$. The Jacobi equation (5.9) in this case reads

$$w'' - 5w' \tan \phi + 4w \tan^2 \phi = \mu \sec^6 \phi.$$

Its fundamental and particular solutions and auxiliary functions read,

$$\begin{aligned}\bar{w}_1 &= \tan \phi \sec \phi, & \bar{w}_2 &= \sec^2 \phi - T(\phi)\bar{w}_1, & T(\phi) &= \ln(\tan \phi + \sec \phi), \\ \bar{w}_3 &= -\frac{\sec^4 \phi}{2} + \frac{3}{4}\bar{w}_1 [T(\phi) + \bar{w}_1], & I_2(\phi) &= \frac{T(\phi)}{4} [3 - 4I_1(\phi)] + \frac{3}{4}\bar{w}_1, \\ I_1(\phi) &= \frac{\sec^2 \phi}{2}, & I_3(\phi) &= \frac{3T(\phi)}{32} [8I_1(\phi) - 5] + \frac{\bar{w}_1}{32} [4I_1(\phi) - 15].\end{aligned}\quad (5.12)$$

The determinant $\Delta_{cat}(\phi_1, \phi_2) = \Delta_{cat}$ is given by

$$\frac{32\Delta_{cat}}{K_{12}} = T_{12}(7M_3 - 2M_5 - 6M_1) - [3T_{12}^2 - 3L_2 + 4L_4]J_{12} + (L_2 - 2)(2L_2 - 3)K_{12},$$

where $T_{12} = T(\phi_1) - T(\phi_2)$, $J_{12} = \tan \phi_1 \tan \phi_2$, $K_{12} = \sec \phi_1 \sec \phi_2$, and

$$L_n = \sec^n \phi_1 + \sec^n \phi_2, \quad M_n = \tan \phi_1 \sec^n \phi_2 - \tan \phi_2 \sec^n \phi_1.$$

Matrix elements P_{ij} calculated from (4.11) are too cumbersome to be presented here. Functions $\eta(\phi_j, \psi_j^*)$ and $K(\phi_j, \psi_j)$ are calculated substituting (5.10) into (5.3, 5.7).

5.1.1 Cat meniscus between two plates

The Cat with given endpoints on two solid plates exists for arbitrary contact angles θ_j . Parametrization of plates and relations between ϕ_j and θ_j read (see Figure 3(a))

$$R_j = A\psi_j, \quad Z_j = d_j, \quad \theta_j = \frac{\pi}{2} + (-1)^j \phi_j, \quad \eta_j = A \sec \phi_j, \quad 2K_j = -A^2 \sin \phi_j \cos^2 \phi_j.$$

By (5.5) the critical angles ϕ_j^\bullet read: $\phi_j^\bullet = (-1)^{j+1} \pi/2$, that makes every point of infinite plates (at the distance $d = d_1 - d_2$) attainable by Cat meniscus.

In Figure 3(a) the red curve determines the boundaries of $\text{Stab}_1(\phi_1, \phi_2)$ defined in (3.15) while the lower boundary of stability domain gives the boundaries of $\text{Stab}_2(\phi_1, \phi_2)$ defined in (4.14). Numerical calculations show a nice coincidence with boundaries found in the framework of Vogel's approach in [24],

$$5 \int_{\phi_1}^{\phi_2} \cos^{-5} t \, dt \cdot \int_{\phi_1}^{\phi_2} \cos^{-1} t \, dt = 9 \left(\int_{\phi_1}^{\phi_2} \cos^{-3} t \, dt \right)^2. \quad (5.13)$$

In symmetric setup (4.17) Cat meniscus between two plates is stable if $\theta \geq 14.97^\circ$.

5.1.2 Cat meniscus between two ellipsoids

Consider Cat meniscus between two axisymmetric ellipsoids given by equation $R_j^2 + (Z_j - g_j)^2 \epsilon_j^{-2} = A^2$, $\epsilon_j > 0$, where ϵ_j stands for anisotropy parameter and $\{0, g_j\}$ denotes coordinates of the j -th ellipsoid

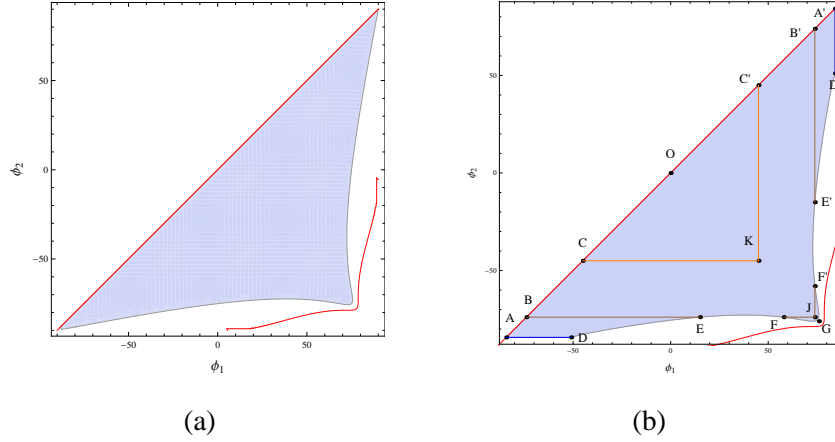


Figure 3: (a) Stability diagram (*SD*) for Cat menisci between two plates in a halfplane $\phi_1 > \phi_2$ is shaded in gray. (b) The *SD* for Cat menisci between two equal spheres are represented by interiors of polygons: $A = 100$, $\{OCBADEFGF'E'D'A'B'C'O\}$, $\phi^\bullet(1, 100) = 84.3^\circ$; $A = 13$, $\{OCBEFJF'E'A'B'C'O\}$, $\phi^\bullet(1, 13) = 73.9^\circ$; $A = 4$, $\{OCKC'O\}$ $\phi^\bullet(1, 4) = 60^\circ$. The *red curves* show the location of conjugate points while the *blue lines* show the location of points where $\eta(\phi_j^\bullet, \psi_j^*) = 0$, $\sec \phi_j^\bullet = 100 \sin \psi_j^*$.

center. Ellipsoids may be specified as prolate ($\epsilon_j > 1$) and oblate ($\epsilon_j < 1$). The upper and lower ellipsoids are separated by distance $d = g_1 - g_2 - A(\epsilon_1 + \epsilon_2)$ and given parametrically,

$$R_j = A \sin \psi_j, \quad Z_j = g_j + (-1)^j A \epsilon_j \cos \psi_j, \quad \eta_j = \frac{\sqrt{A^2 \cos^2 \phi_j - 1} + (-1)^j \epsilon_j \tan \phi_j}{\cos^2 \phi_j},$$

$$K_j = -\frac{\eta_j \cos \phi_j}{2} \left(\eta_j \sin \phi_j \cos^3 \phi_j + (-1)^j \epsilon_j \left[1 + \frac{1}{\cos^2 \phi_j + \epsilon_j^2 \sin^2 \phi_j} \right] \right).$$

According to (5.4) the contact angles are given by

$$\theta_j = \frac{\pi}{2} + (-1)^j \phi_j - \arctan \frac{\epsilon_j}{\sqrt{A^2 \cos^2 \phi_j - 1}}.$$

By (5.5) the critical angles $\phi_j^\bullet = \phi_j^\bullet(\epsilon_j, A)$ are given by equation,

$$A^2 \cos^4 \phi_j^\bullet + (\epsilon_j^2 - 1) \cos^2 \phi_j^\bullet - \epsilon_j^2 = 0, \quad \phi_1^\bullet(1, A) = -\phi_2^\bullet(1, A) = \arccos \frac{1}{\sqrt{A}}, \quad (5.14)$$

where $\epsilon_j = 1$ stands for two equal spheres. This makes the areas, attainable by Cat stable meniscus on the spheres, substantially limited. Figure 3(b) shows stability diagrams (*SD*) of Cat menisci between two equal spheres of different radii. Decrease of A reduces the stability domain $\text{Stab}_2(\phi_1, \phi_2)$ caused by non-planar solid bodies and decrease of ϕ_j^\bullet . For $A < 11.7$ the domain $\text{Stab}_2(\phi_1, \phi_2)$ is a right isosceles triangle $\{OCKC'O\}$, otherwise the domain has curvilinear boundaries.

5.1.3 Cat meniscus between other solid bodies

The theory of PR stability with free CL developed in section 4 can be applied to arbitrary pair of axisymmetric solid bodies. Here we study another pair, two paraboloids. Consider the Cat meniscus between two convex parts of axisymmetric solid bodies,

$$R_j = A\psi_j, \quad Z_j = g_j + (-1)^{j+1}AC_ja_j(\psi_j/a_j)^{\nu_j}, \quad a_j, \nu_j, C_j, A > 0. \quad (5.15)$$

For $\nu_j > 1$ the surface is smooth at $\psi_j = 0$, otherwise it has a singularity point. The case $\nu_j = 1$

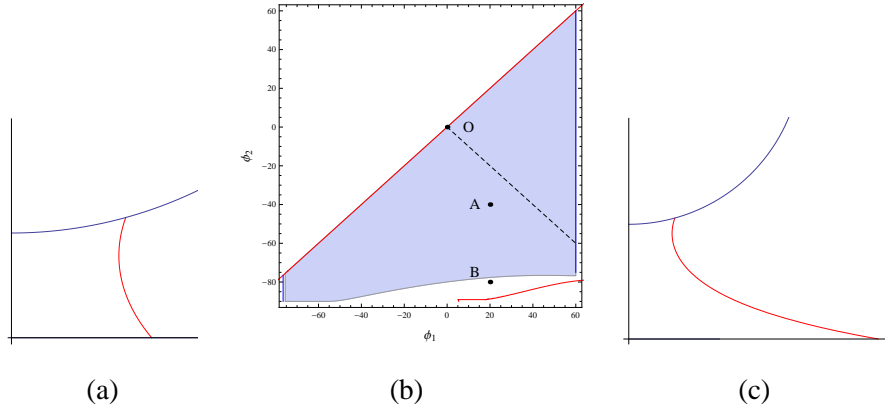


Figure 4: The *SD* (b) for Cat menisci between solid plate and sphere, $A = 4$, is not symmetric w.r.t. the *dashed* line $\phi_1 + \phi_2 = 0$. The critical angles are $\phi_1^\bullet(1, 4) = 60^\circ$, $\phi_2^\bullet(0, 4) = -75.5^\circ$. Points *A* and *B* mark (a) stable $\phi_1 = 20^\circ$, $\phi_2 = -40^\circ$, and (c) unstable $\phi_1 = 20^\circ$, $\phi_2 = -80^\circ$, menisci, respectively.

represents a conic surface. The critical angles ϕ_j^\bullet are given by relations,

$$\nu_j C_j \tan \phi_j^\bullet = (a_j A \cos \phi_j^\bullet)^{\nu_j - 1}, \quad \nu_j > 1; \quad \cot \phi_j^\bullet = C_j, \quad \nu_j = 1.$$

When Cat meniscus connects solid bodies of different shape the stability domain loses its symmetry w.r.t. the line $\phi_1 + \phi_2 = 0$, thus breaking an equality $\phi_1^\bullet = -\phi_2^\bullet$ for critical angles. This can be seen in the setup of meniscus between solid sphere and plate at Figure 4, for which according to (5.14) we have,

$$\phi_1^\bullet(1, A) = \arccos \frac{1}{\sqrt{A}}, \quad \phi_2^\bullet(0, A) = -\arccos \frac{1}{A}.$$

6 Pendular rings with nonzero curvature

For $H \neq 0$ the equation (5.2) is solved in elliptic integrals of the first *F* and the second *E* kind. Here we choose a parametrization similar to that used in [9],

$$\bar{r}(\phi) = \sqrt{1 + B^2 + 2B \cos \phi}, \quad \bar{z}(\phi) = M(\phi, B) - M(\phi_2, B) + Z_2(\psi_2), \quad (6.1)$$

$$M(\phi, B) = (1 + B)E(\phi/2, m) + (1 - B)F(\phi/2, m), \quad m^2 = \frac{4B}{(1 + B)^2},$$

where m stands for modulus of elliptic integral. The expression for B is given by

$$B^2 + 2B \cos \phi_1 + 1 = R_1^2(\psi_1).$$

The solution derivatives satisfy the relationships

$$\frac{\bar{r}'}{B} = -\frac{\sin \phi}{\bar{r}}, \quad \frac{\bar{r}''}{B} = \frac{\bar{r}' \sin \phi}{\bar{r}^2} - \frac{\cos \phi}{\bar{r}}, \quad \bar{z}' = \frac{1 + B \cos \phi}{\bar{r}}, \quad \bar{z}'' = \frac{\bar{r}'(\bar{r} - \bar{z}')}{\bar{r}}. \quad (6.2)$$

Formulas (6.1) describe four Delaunay's types [5] of surfaces of revolution with constant H : *cylinder* (Cyl), $B = 0$, *unduloid* (Und), $B < 1$, *sphere* (Sph), $B = 1$, and *nodoid* (Nod), $B > 1$. Entries in (2.17) read,

$$H_1 = H_3 = \bar{r}, \quad H_2 = -(\bar{r} + 2\bar{r}''), \quad L = \bar{r}' - \bar{z}'\bar{z}''\bar{r}, \quad N = -\bar{r}'\bar{r}''\bar{r}, \quad M = \bar{z}'\bar{r}''\bar{r}.$$

Note that $\bar{r}'^2 + \bar{z}'^2 = 1$, and H_1 is positive as in section 5.1. Equation (5.9) reads

$$w'' - \frac{B \sin \phi}{\bar{r}^2} w' + \left(1 - \frac{2B \cos \phi}{\bar{r}^2} - \frac{2B^2 \sin^2 \phi}{\bar{r}^4}\right) w = \mu. \quad (6.3)$$

Its fundamental and particular solutions and corresponding auxiliary functions read:

$$\begin{aligned} \bar{w}_1 &= \frac{\sin \phi}{\bar{r}}, \quad \bar{w}_2 = \cos \phi + (1 + B)M_1\bar{w}_1, \quad \bar{w}_3 = 1 + (1 + B)M_2\bar{w}_1, \\ I_1 &= -\cos \phi, \quad \eta_j = \frac{1}{\bar{r}(\phi_j)} \left[(1 + B \cos \phi_j)R_j'(\psi_j^*) + B \sin \phi_j Z_j'(\psi_j^*) \right], \\ I_2 &= \bar{r} \sin \phi + (1 + B)(I_1 M_1 + M_2), \quad I_3 = (1 + B) \left[2E\left(\frac{\phi}{2}, m\right) + I_1 M_2 + M_1 \right] \\ M_1(\phi, m) &= E\left(\frac{\phi}{2}, m\right) - F\left(\frac{\phi}{2}, m\right) + M_2, \quad M_2(\phi, m) = \frac{m^2}{2} F\left(\frac{\phi}{2}, m\right). \end{aligned}$$

Expression for $\Delta(\phi_1, \phi_2)$ for arbitrary meniscus of nonzero curvature is too long to be presented here.

6.1 Stability of cylinder menisci Cyl

Specify the above formulas for Cyl meniscus,

$$\begin{aligned} B &= 0, \quad \bar{r} = 1, \quad \bar{z} = \phi, \quad \bar{w}_1 = \sin \phi, \quad \bar{w}_2 = \cos \phi, \quad \bar{w}_3 = 1, \quad L = M = N = 0, \\ I_1 &= -\cos \phi, \quad I_2 = \sin \phi, \quad I_3 = \phi, \quad \eta_j = R_j'(\psi_j^*), \quad K_j = \xi_j. \end{aligned} \quad (6.4)$$

Expressions for $\Delta_{Cyl}(\phi_1, \phi_2)$ and matrix elements P_{ij} read

$$\begin{aligned} \Delta_{Cyl}(\phi_1, \phi_2) &= \Delta\phi \Gamma_1 \left(\frac{\Delta\phi}{2} \right) \sin \Delta\phi, \quad \Gamma_1(x) = 1 - \frac{\tan x}{x}, \quad \Delta\phi = \phi_1 - \phi_2, \\ P_{11} = P_{22} &= \Delta\phi \Gamma_1(\Delta\phi) \cos \Delta\phi, \quad P_{12} = -\Delta\phi \Gamma_2(\Delta\phi), \quad \Gamma_2(x) = 1 - \frac{\sin x}{x}. \end{aligned}$$

6.1.1 Cyl meniscus between two plates

We have $\theta_1 = \theta_2 = \pi/2$ and $R_j = \psi_j$, $Z_j = d$, $K_j = 0$, leading to

$$Q_{11} = Q_{22} = \frac{\Gamma_1(\Delta\phi)}{\Gamma_1(\Delta\phi/2)} \cot \Delta\phi, \quad Q_{12} = -\frac{\Gamma_2(\Delta\phi)}{\Gamma_1(\Delta\phi/2)} \csc \Delta\phi, \quad Q_{33} = -\frac{1}{\Gamma_1(\Delta\phi/2)}.$$

There are no conjugate points in region $\Delta_{Cyl}(\phi_1, \phi_2) < 0$, i.e., $\Delta\phi < 2\pi$. The stability domains $\text{Stab}(\Delta\phi)$ for three different BCs are the following

- (a) fixed endpoints : $\Delta_{Cyl} < 0 \Rightarrow 0 < \Delta\phi < 2\pi$,
- (b) one endpoint is free and another is fixed : $Q_{11} > 0 \Rightarrow 0 < \Delta\phi < \varkappa\pi$,
- (c) free endpoints : $Q_{33} > 0 \Rightarrow 0 < \Delta\phi < \pi$,

where $\varkappa = \min\{x_* \mid \tan x_* = x_*, x_* > 0\} \simeq 1.4303$. Stability of Cyl meniscus between two plates is well studied and often compared [18], [11] to the Plateau-Rayleigh instability of a slow flowing liquid jet of infinite length. Its threshold coincides with the case (a) above in the following sense: the jet of the circular cross-section is stable if the length of fluctuations does not exceed the circumference.

6.1.2 Cyl meniscus between two ellipsoids or plate and ellipsoid

Using parametrization of section 5.1.2 allow anisotropy ϵ to get both positive and negative values that distinguishes the exterior (convex) ellipsoid shape ($\epsilon > 0$) and its interior (concave, or hollow) shape ($\epsilon < 0$),

$$\frac{Q_{jj}}{A^2} = \frac{\epsilon_j \sin \psi_j^* \cos \psi_j^*}{\epsilon_j^2 \sin^2 \psi_j^* + \cos^2 \psi_j^*} + \frac{P_{jj} \cos^2 \psi_j^*}{\Delta_{Cyl}}, \quad \frac{Q_{12}}{A^2} = \frac{P_{12} \cos \psi_1^* \cos \psi_2^*}{\Delta_{Cyl}},$$

where P_{ij} are given in section 6.1. Consider a case of Cyl between equal ellipsoids. The stability criteria (4.11) give rise to the *SD* boundaries by equation,

$$\cot \frac{\Delta\phi}{2} + \frac{\epsilon \tan \psi^*}{\epsilon^2 \sin^2 \psi^* + \cos^2 \psi^*} = 0, \quad (6.5)$$

that results in solutions for spheres (see Figure 5(a), for $\epsilon = 1$ it coincides with that of reported in [20],

$$\psi^* = \frac{-\pi + \Delta\phi}{2}, \quad 1 \leq \frac{\Delta\phi}{\pi} \leq 2 \quad \text{and} \quad \psi^* = \frac{\pi - \Delta\phi}{2}, \quad 0 \leq \frac{\Delta\phi}{\pi} \leq 1.$$

The case of Cyl meniscus between the plate and ellipsoid gives,

$$\frac{Q_{11}}{A^2} = \frac{\epsilon \sin \psi^* \cos \psi^*}{\epsilon^2 \sin^2 \psi^* + \cos^2 \psi^*} + \frac{P_{11} \cos^2 \psi^*}{\Delta_{Cyl}}, \quad \frac{Q_{22}}{A^2} = \frac{P_{22}}{\Delta_{Cyl}}, \quad \frac{Q_{12}}{A^2} = \frac{P_{12} \cos \psi^*}{\Delta_{Cyl}}.$$

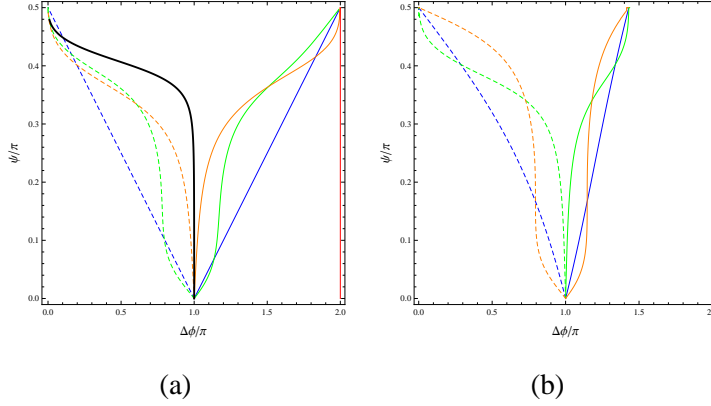


Figure 5: (a) The right boundaries of SD for Cyl menisci between two solid (*plain*) and hollow (*dashed*) ellipsoids shown in *blue*: $\epsilon_j = 1(-1)$, *green*: $\epsilon_1 = 3(-3)$, $\epsilon_2 = 0.1(-0.1)$, and *orange*: $\epsilon_1 = 0.05(-0.05)$, $\epsilon_2 = 0.15(-0.15)$. The *thick black curve* corresponds to Cyl meniscus between solid and hollow ellipsoids ($\epsilon_1 = -\epsilon_2 = 0.05$). (b) The right boundaries of SD for Cyl menisci between plate and convex (*plain*) or hollow (*dashed*) ellipsoids shown in *blue*: $\epsilon_1 = \epsilon_2 = 1(-1)$, *orange*: $\epsilon_1 = \epsilon_2 = 3(-3)$, and *green*: $\epsilon_1 = \epsilon_2 = 0.1(-0.1)$. The left boundary of SD in both Figures (a,b) coincides with the ψ axis.

Its stability is governed by equation,

$$\frac{\tan(\Delta\phi)}{\Gamma_1(\Delta\phi)} - \frac{\epsilon \tan \psi^*}{\epsilon^2 \sin^2 \psi^* + \cos^2 \psi^*} = 0, \quad (6.6)$$

that results in solutions for sphere ($\epsilon = 1$) upon the plate (see Figure 5(b)),

$$\cot \psi^* = \cot \Delta\phi - \frac{1}{\Delta\phi}, \quad 1 \leq \frac{\Delta\phi}{\pi} \leq \varkappa, \quad \cot \psi^* = \frac{1}{\Delta\phi} - \cot \Delta\phi, \quad 0 \leq \frac{\Delta\phi}{\pi} \leq 1.$$

6.1.3 Cyl meniscus between two paraboloids or two catenoids

Using parametrization (5.15) write a matrix Q_{ij} and the governing equation for stability of Cyl between two equal paraboloids, $C_i = C$, $a_i = a$, $\nu_i = \nu$ (see Figure 6(a)),

$$\frac{Q_{jj}}{A^2} = \rho \frac{\nu - 1}{1 + \rho^2} + \frac{P_{jj}}{\Delta_{Cyl}}, \quad \frac{Q_{12}}{A^2} = \frac{P_{12}}{\Delta_{Cyl}}, \quad \rho = \frac{C\nu}{a^{\nu-1}}, \quad \cot \frac{\Delta\phi}{2} + \rho \frac{\nu - 1}{1 + \rho^2} = 0.$$

The Cyl meniscus between two solid catenoids,

$$R_j = A\psi_j, \quad Z_j = g_j + (-1)^{j+1} AC_j \cosh(b_j\psi_j), \quad C_j, b_j, A > 0, \quad (6.7)$$

in the case of equal catenoids, $C_j = C$, $b_j = b$, produces (see Figure 6(b))

$$\frac{Q_{jj}}{A^2} = \frac{Cb^2 \cosh b}{1 + C^2 b^2 \sinh^2 b} + \frac{P_{jj}}{\Delta_{Cyl}}, \quad \frac{Q_{12}}{A^2} = \frac{P_{12}}{\Delta_{Cyl}}, \quad \cot \frac{\Delta\phi}{2} + \frac{Cb^2 \cosh b}{1 + C^2 b^2 \sinh^2 b} = 0.$$

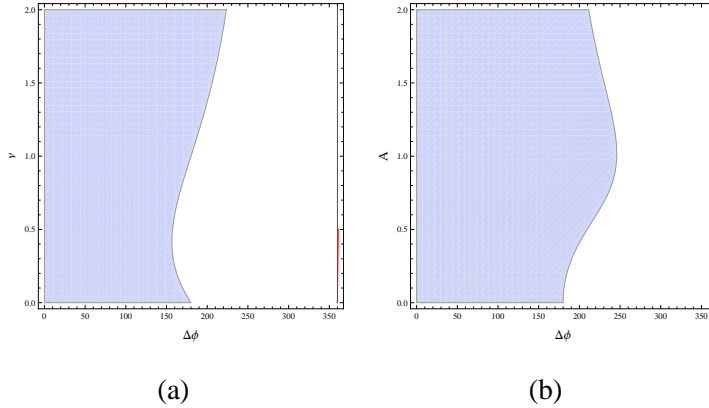


Figure 6: The SD for Cyl meniscus between (a) two solid paraboloids for $a_i = C_i = 1$, $\nu_1 = \nu_2 = \nu$, and (b) two solid catenoids for $C_i = 1$, $b_1 = b_2 = b$.

6.2 Stability of nonzero curvature menisci between two plates

In a variety of axisymmetric menisci with $H \neq 0$ between two solid bodies we focus on the simple case of two plates and present $\text{Stab}_2(\phi_1, \phi_2)$ for all menisci types. An importance of the two plates setup is based on the statement [7]: *every stable connected configuration is rotationally symmetric, i.e., axisymmetric PR between two plates under 3D non-axisymmetric perturbations do not bifurcate to any stable 3D non-axisymmetric PR*. The stability triangle for Sph menisci in Figure 7 (b) describes a single Sph segment trapped between two plates. Its right corner $\phi_1 = -\phi_2 = 180^\circ$ corresponds to the whole sphere with contact angles $\theta_1 = \theta_2 = \pi$ embedded between two plates. The SD for Und menisci in Figure 7 (c,d) are intermediate domains in the range $0 < B < 1$ between Cyl and Sph menisci. The existence of IP in the Und meridional profile \mathcal{M}_U is governed by requirement:

$$\phi_2 \leq \phi_U^{ip} \leq \phi_1, \quad \bar{z}'(\phi_U^{ip})\bar{r}''(\phi_U^{ip}) - \bar{z}''(\phi_U^{ip})\bar{r}'(\phi_U^{ip}) = 0 \Rightarrow \cos \phi_U^{ip} = -B.$$

A value ϕ_U^{ip} has important property, namely, from (4.12) we obtain

$$Q_{33}(\phi_U^{ip}, -\phi_U^{ip}) = 0. \quad (6.8)$$

In section 6.2.1 we give detailed discussion of ϕ_U^{ip} relationship to Und stability.

The SD for Nod menisci in Figure 8 differs from the rest of diagrams and comprise two different sort of sub-diagrams: Nod menisci with convex and concave meridional profiles \mathcal{M}_N . The positive curvature H corresponds to the convex part of \mathcal{M}_N , while the negative H produces its concave segment. This justifies the non-existence of Nod meniscus with both its convex and concave parts which meet at ϕ_N^{ip} such that $z'(\phi_N^{ip}) = 0$, i.e., $\cos \phi_N^{ip} = -B^{-1}$.

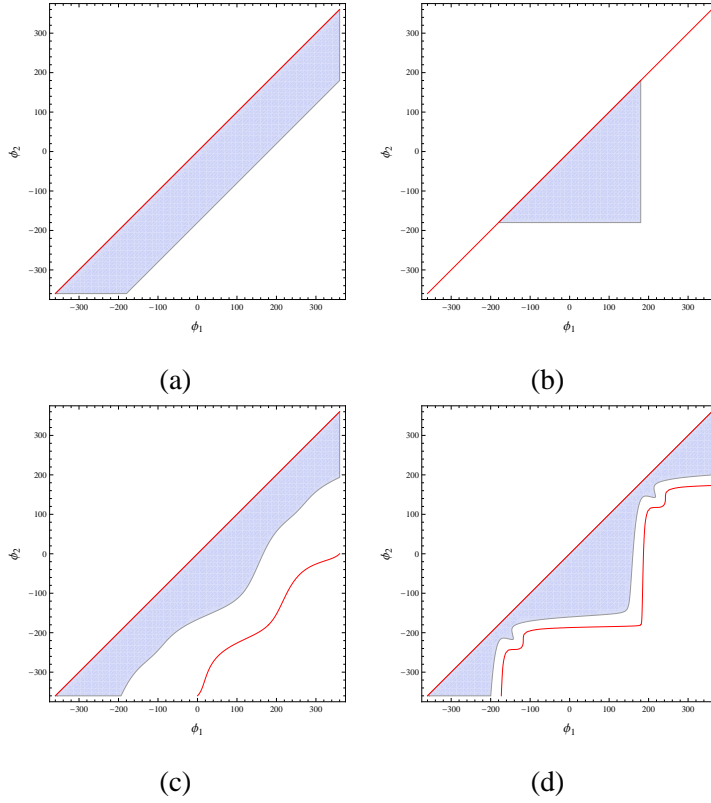


Figure 7: The SD for (a) Cyl, $B = 0$, (b) Sph, $B = 1$, and two Und menisci, (c) $B = 0.3$ and (d) $B = 0.8$, between two plates. The red curves in (c.d) show the location of conjugate points.

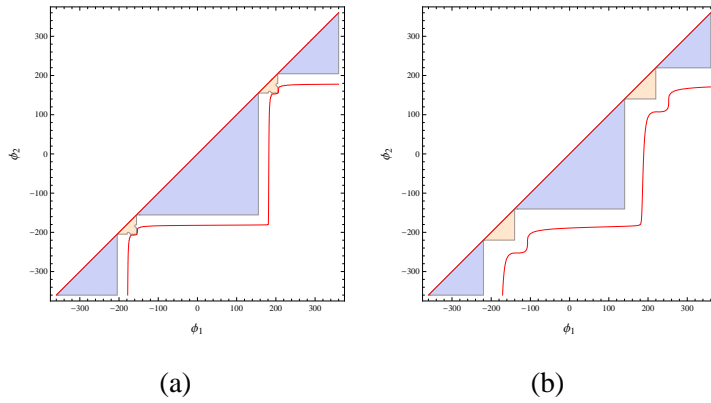


Figure 8: The SD for Nod menisci between two plates, with (a) $B = 1.1$ and (b) $B = 1.3$. Different types of Nod menisci curvature are shown in *violet-blue* (positive) and *orange* (negative) colors.

6.2.1 Und menisci with inflection point between two plates

In this section we verify three statements [1], [18], [19], [7] about stability of Und menisci with free contact points between two plates with contact angles θ_1, θ_2 . We also present a new statement summarizing

our investigations on stability domain.

1. If $\theta_1 = \theta_2 = \pi/2$ the Und menisci are unstable [1], [18].

The Und menisci with such BC have necessarily one or more *IPs*: one *IP* for $\phi_1 = n\pi, \phi_2 = (n-1)\pi$, two *IPs* if $\phi_1 = n\pi, \phi_2 = (n-2)\pi$, etc., where n is an integer. However, for $n \geq 2$ a criterion (3.14) is broken, i.e., the conjugate points appear. So there remains one *IP* and a direct calculation of Q_{33} gives for $0 < m < 1$,

$$4 \frac{Q_{33}(0, -\pi)}{(1-B)^2} = [3E(m) - K(m)][E(m) - K(m)] + m^2 K(m)[2E(m) - K(m)] < 0,$$

where $K(m)$ and $E(m)$ denote the complete elliptic integral of the first and second kind. The last inequality may be verified numerically. In Figure 9 we present detailed locations of Und menisci with $B = 0.3$ in the sense of its stability w.r.t. the boundaries $\Delta(\phi_1, \phi_2) = 0$ (the red curve \mathfrak{R}) and $Q_{33}(\phi_1, \phi_2) = 0$ (the gray curve \mathfrak{G}). The points $C(\phi_1 = 0, \phi_2 = -\pi)$ and $C'(\phi_1 = \pi, \phi_2 = 0)$ lie in unstable zone.

2. If $\theta_1 = \theta_2$ there are no stable menisci with one or more *IPs* [7], Theorem 5.7.

All Und menisci with $\theta_1 = \theta_2$ and without *IP* have the endpoints satisfying $\phi_1 + \phi_2 = 0$. In Figure 9 they belong to the interval OD of the blue line \mathfrak{B} and are stable. There are two different ways to generate *IP*.

First, allow ϕ_1 to grow by preserving the above equality that leaves the meniscus symmetric w.r.t. reflection plane between two plates. When $\phi_1 = \phi_U^{ip}$ there appears a couple of *IPs* (see Figure 9(b)), i.e., *IPs* are born on both plates simultaneously. We cannot make any conclusion about stability of this meniscus in the framework of Weierstrass' theory. But all menisci with $\phi_1 + \phi_2 = 0, \phi_1 > \phi_U^{ip}$, having two *IPs* are unstable. In Figure 9 they belong to \mathfrak{G} beyond the point D. Thus, the range of equal contact angles θ for stable menisci without *IP* reads, $\pi/2 < \theta < \phi_U^{ip}$ for convex Und and $\pi - \phi_U^{ip} < \theta < \pi/2$ for concave Und.

Another way to generate *IP* with $\theta_1 = \theta_2$ is to break the reflection symmetry $\phi_1 + \phi_2 \neq 0$, where $\phi_1 < \phi_U^{ip}$ and $\phi_2 < -\phi_U^{ip}$. Using (6.2) for $\tan \theta_j = (-1)^{j-1} z'(\phi_j)/r'(\phi_j)$ write an equality for ϕ_1, ϕ_2 ,

$$P(\phi_1) + P(\phi_2) = 0, \quad P(\phi) = \frac{1 + B \cos \phi}{B \sin \phi} \Rightarrow \tan \frac{\phi_1}{2} \tan \frac{\phi_2}{2} = -\frac{1+B}{1-B}. \quad (6.9)$$

Calculation of Q_{33} in accordance to (4.11) and (6.9) leads to a cumbersome expression. Instead of its analysis we present in Figure 9 the blue curve \mathfrak{B} given by equation (6.9) and observe that \mathfrak{B} always lies in instability zone, confirmed by numerical calculation of Q_{33} for $0 < B < 1$. The curves \mathfrak{B} and \mathfrak{G} are tangent at points F, D, H.

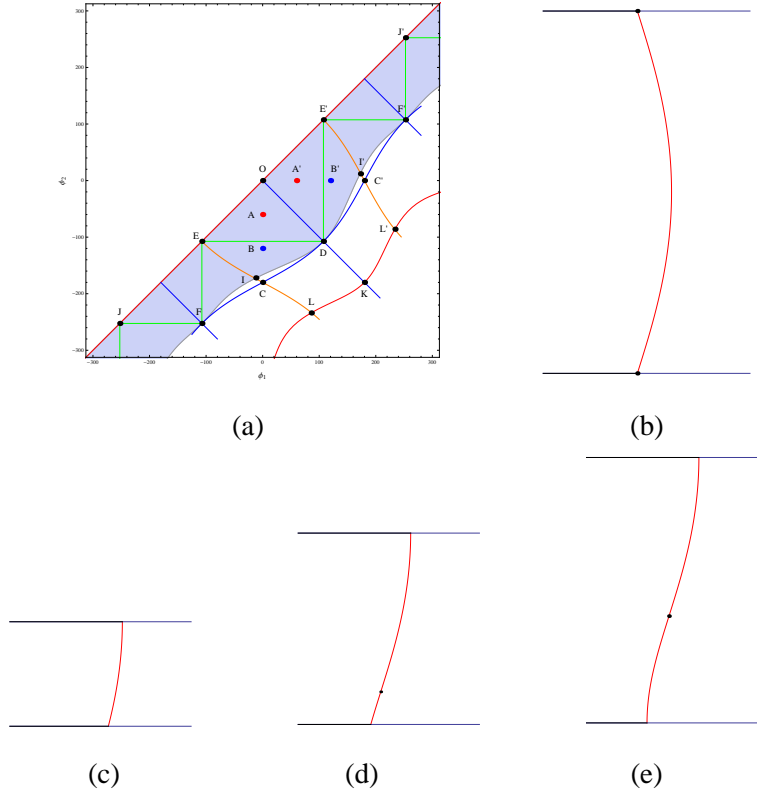


Figure 9: The SD for Und menisci with $B = 0.3$. The green lines \mathfrak{J} show IP separation from a plate. The dots mark menisci shown in: (b) point **D** for $\phi_1 = -\phi_2 = \phi_U^{ip} = 107.46^\circ$ (two IP s at the plates) (c) point **A** for $\phi_1 = 0^\circ, \phi_2 = -60^\circ$ (stable meniscus without IP), (d) point **B** for $\phi_1 = 0^\circ, \phi_2 = -120^\circ$ (stable meniscus with one IP), (e) point **C** for $\phi_1 = 0^\circ, \phi_2 = -180^\circ$ (unstable meniscus with one IP).

There is one more important conclusion: Und meniscus with reflection symmetry ($\theta_1 = \theta_2$) and fixed CL at two plates is stable even when two IP s exist. This follows from an observation that an interval DK at Figure 9 is above the curve \mathfrak{R} . The point $K(\phi_1 = \pi, \phi_2 = -\pi)$ marks unstable Und meniscus of entire period with four IP s when two of them are separated from the plates.

3. If $\theta_1, \theta_2 \neq \pi/2, \theta_1 + \theta_2 = \pi$ there are stable menisci of large volume that have IP s [19], Remark 3.2.

Making use of (6.2) and identity $\tan(\theta_1 + \theta_2) = 0$ write a relation for the angles ϕ_1, ϕ_2 valid for the arbitrary volume's value,

$$P(\phi_1) - P(\phi_2) = 0 \quad \Rightarrow \quad \tan \frac{\phi_1}{2} \tan \frac{\phi_2}{2} = \frac{1+B}{1-B}. \quad (6.10)$$

Similarly to the previous case consider in Figure 9 the brown curves given by equation (6.10) and observe that they always pass through the point **C** and cross transversely the curve \mathfrak{G} at point **I** which separates

the menisci in two families: stable with one IP (at interval GI) and unstable (beyond the point I). Note that the stable menisci without IP are forbidden. Regarding the claim '*stable menisci of large volume that have IPs*' we have found it incorrect. Indeed, the whole segment E'I belongs to the stability region and it remains true when we approach the point E', *i.e.*, when $\phi_2 \rightarrow \phi_1$ that manifests volume decrease up to an arbitrary small value. Therefore we make a statement slightly different: *if $\theta_1 + \theta_2 = \pi$ then only menisci with a single IP are stable.*

Summarize the above results: the stability region $\text{Stab}_2(\phi_1, \phi_2)$ of Und meniscus between two plates with free CL is represented in Figure 9 by interior of domain decomposed in subdomains

$$\text{Stab}_2(\phi_1, \phi_2) = \{DIFE\}_1 \cup \{D'F'E'\}_1 \cup \{JEF\}_0 \cup \{EOE'DE\}_0 \cup \{J'E'F'\}_0$$

where a subscript stands for a number of IP in stable meniscus.

4. Finish this section with two other setups for Und menisci between two plates: $\theta_1 \pm \theta_2 = \pi/2$, which differ from those discussed in [1], [18], [19], [7]. Making use of formulas (6.2) write an equality which is not solvable in ϕ_1, ϕ_2 for all B ,

$$P(\phi_1)P(\phi_2) = \mp 1, \quad |P(\phi)| \geq \left| P\left(\phi_U^{ip}\right) \right| = \frac{\sqrt{1-B^2}}{B}, \quad \Rightarrow \exists \phi_j \in \Re \text{ if } B \geq \frac{1}{\sqrt{2}}.$$

The upper (lower) sign in above equality corresponds to the upper (lower) sign in $\theta_1 \pm \theta_2$. For $B = 1/\sqrt{2}$ there exist two pointwise solutions of equation $P(\phi_1)P(\phi_2) = \mp 1$,

$$a) : \frac{\phi_1}{5} = \frac{\phi_2}{3} = \frac{\pi}{4} \text{ and } \frac{\phi_1}{5} = \frac{\phi_2}{3} = -\frac{\pi}{4}; \quad b) : \frac{\phi_1}{5} = \frac{\phi_2}{5} = \pm \frac{\pi}{4} \text{ and } \frac{\phi_1}{3} = \frac{\phi_2}{3} = \pm \frac{\pi}{4}.$$

However, when $B > 1/\sqrt{2}$ the solutions are represented by curves L_a and L_b in the halfplane $\{\phi_2 < \phi_1\}$: L_a passes through unstable and stable (without IP) zones while L_b exists only in stable zones with and without IP (see Figure 10).

Acknowledgement

The useful discussions with O. Lavrenteva are appreciated. The research was supported in part (LGF) by the Kamea Fellowship.

References

- [1] M. ATHANASSENAS, *A variational problem for constant mean curvature surfaces with free boundary*, J. für Math., **377** (1987), pp. 97-107.

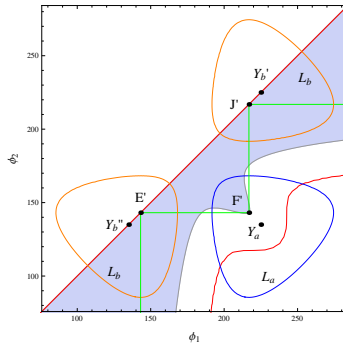


Figure 10: The SD for Und menisci with $B = 0.8$ (a part of Figure 7(d)). The *green* line shows the position of IPs . The dots mark menisci contacting the lower and upper plates at ϕ_2 and ϕ_1 , respectively: (Y_a) $\phi_1 = 225^\circ, \phi_2 = 135^\circ$, (Y_b') $\phi_1 = \phi_2 = 225^\circ$, (Y_b'') $\phi_1 = \phi_2 = 135^\circ$, in accordance with section 6.2.1. Curves L_a and L_b describe Und menisci satisfying $\theta_1 + \theta_2 = \pi/2$ and $\theta_1 - \theta_2 = \pi/2$, respectively.

- [2] A. BEER, *Tractatus de Theoria Mathematica Phenomenorum in Liquidis Actioni Gravitatis Delectis Observatorum*, George Carol, Bonn, 1857.
- [3] O. BOLZA, *Lectures on the Calculus of Variations*, Univ. Chicago Press, 1904.
- [4] R. COURANT AND D. HILBERT, *Methods of mathematical physics*, **1**, New York: Wiley, 1989.
- [5] C.E. DELAUNAY, *Sur la surface de révolution dont la courbure moyenne est constante*, J. Math. Pure et App., **16** (1841), pp. 309-315.
- [6] M.A. ERLE, R.D. GILLETTE AND D.C. DYSON, *Stability of interfaces of revolution - the case of catenoid*, Chem. Eng. J., **1** (1970), pp. 97-109.
- [7] R. FINN AND T. VOGEL, *On the volume infimum for liquid bridges*, Zeitschrift für Analysis und ihre Anwendungen, **11** (1992), pp. 3-23.
- [8] R.D. GILLETTE AND D.C. DYSON, *Stability of fluid interfaces of revolution between equal solid plates*, Chem. Eng. J., **2** (1971), pp. 44-54.
- [9] M. HADZHILAZOVA, I. MLADENOV AND J. OPREA, *Unduloids and their geometry*, Archivum Mathematicum, **43** (2007), pp. 417-429.
- [10] W. HOWE, *Die Rotations-Flächen welche bei vorgeschriebener Flächengrösse ein möglichst grosses oder kleines Volumen enthalten*, Inaug.-Dissert., Friedrich-Wilhelms-Univ. zu Berlin, 1887.

- [11] D. LANGBEIN, *Capillary Surfaces: shape - stability - dynamics, in particular under weightlessness*, Springer Tracts in Modern Physics, **178**, New York, Paris, Tokyo: Springer, 2002.
- [12] A.D. MYSHKIS, V.G. BABSKII, N.D. KOPACHEVSKII, L.A. SLOBOZHANIN AND A.D. TYUPTSOV, *Lowgravity Fluid Mechanics*, Springer, New York, 1987.
- [13] F. M. ORR, L. E. SCRIVEN AND A. P. RIVAS, *Pendular rings between solids: meniscus properties and capillary forces*, J. Fluid Mech., **67** (1975), pp. 723-744.
- [14] J. A. F. PLATEAU, *Statique expérimentale et théorique des liquides*, Gauthier-Villars, Paris, 1873.
- [15] B.Y. RUBINSTEIN AND L.G. FEL, *Theory of Axisymmetric Pendular Rings*, J. Colloid Interf. Sci., **417** (2014), pp. 37-50.
- [16] D. STRUBE, *Stability of spherical and catenoidal liquid bridge between two parallel plates in absence of gravity*, Micrograv. Sci. Technol., **4** (1991), pp. 263-269.
- [17] M. STURM, *Note, Á l'occasion de l'article précédent*, J. Math. Pure et App., **16** (1841), pp. 315-321.
- [18] T. VOGEL, *Stability of a liquid drop trapped between two parallel planes*, SIAM J. Appl. Math., **47** (1987), pp. 516-525.
- [19] T. VOGEL, *Stability of a liquid drop trapped between two parallel planes, II: General contact angles*, SIAM J. Appl. Math., **49** (1989), pp. 1009-1028.
- [20] T. VOGEL, *Non-linear stability of a certain capillary problem*, Dynamics of Continuous, Discrete and Impulsive Systems, **5** (1999), pp. 1-16.
- [21] T. VOGEL, *Convex, rotationally symmetric liquid bridges between spheres*, Pacific J. Math., **224** (2006), pp. 367-377.
- [22] K. WEIERSTRASS, *Mathematische Werke von Karl Weierstrass, 7, Vorlesungenüber Variationsrechnung*, Leipzig, Akademische Verlagsgesellschaft, 1927.
- [23] H.C. WENTE, *The symmetry of sessile and pendant drops*, Pacific J. Math., **88** (1980), pp. 387-397
- [24] L. ZHOU, *On stability of a catenoidal liquid bridge*, Pacific J. Math. **178** (1997), pp. 185-198.